3

Statistically Self-Similar Signals

3.1 INTRODUCTION

Some of the most prevalent forms of fractal geometry in nature arise out of statistical scaling behavior in the underlying physical phenomena. In this chapter, we study an important class of statistically scale-invariant or self-similar random processes known as $1/f$ processes. These empirically defined processes, in particular, model a wide range of natural signals.

In the first half of this chapter we first review the empirical properties of $1/f$ processes and a traditional mathematical model for $1/f$ behavior based on the fractional Brownian motion framework of Mandelbrot and Van Ness [39]. We then introduce and study an alternative mathematical characterization for $1/f$ processes. The novelty and power of this characterization are its basis in the frequency domain, which admits a broader range of Fourier tools in the analysis of $1/f$ processes. In addition, we are able to show that our characterization includes the models of Mandelbrot and Van Ness, yet appears to avoid some of their limitations.

The latter half of the chapter develops models for a more broadly defined class of *nearly*-$1/f$ models, which constitute equally useful models for many natural signals. For completeness, we first review some well-known ARMA-based constructions for nearly-$1/f$ processes. However, the principal focus in this section is on developing some powerful and efficient *wavelet-based* nearly-$1/f$ models. Using our frequency-based characterization of $1/f$ processes, we are able to show that a rather broad class of wavelet bases yield Karhunen-Loève-like expansions for nearly-$1/f$ processes. As a consequence, it is reasonable to model $1/f$ processes as orthonormal wavelet basis expansions in terms of uncorrelated coefficients. This suggests that wavelet-based analysis of $1/f$-type behavior is not only convenient, but, in an appropriate sense, statistically optimal. In fact, in Chapter 4 we show how these wavelet-based representations are extremely useful in addressing problems of optimum detection and estimation involving $1/f$-type signals.

Before proceeding with our development, we point out that a basic engineering background in probability, random variables, and random processes is assumed of the reader throughout this chapter. Useful treatments of this background material can be found in, e.g., Papoulis [40] or Stark and Woods [41].

We begin with a rather universally accepted definition. A random process $x(t)$ defined on $-\infty < t < \infty$ is said to be ***statistically self-similar*** if its statistics are invariant to dilations and compressions of the waveform in time. More specifically, a random process $x(t)$ is statistically self-similar with parameter H if for any real $a > 0$ it obeys the scaling relation

$$x(t) \stackrel{p}{=} a^{-H} x(at) \tag{3.1}$$

where $\stackrel{p}{=}$ denotes equality in a statistical sense. For ***strict-sense*** self-similar processes, this equality is in the sense of all finite-dimensional joint probability distributions. For *wide-sense* self-similar processes, the equality may be interpreted in the sense of second-order statistics, i.e., mean and covariance functions. In this latter case, the self-similarity relation (3.1) may be alternately expressed as

$$M_x(t) \stackrel{\Delta}{=} E[x(t)] = a^{-H} M_x(at) \tag{3.2a}$$

$$R_x(t,s) \stackrel{\Delta}{=} E[x(t)x(s)] = a^{-2H} R_x(at, as). \tag{3.2b}$$

We restrict our attention to Gaussian processes, for which the two definitions are equivalent. Furthermore, we consider only zero-mean processes.

Even Gaussian processes satisfying (3.1) can exhibit great diversity in behavior. Some are stationary, as is the case with the classical generalized process $w(t)$ corresponding to zero-mean, stationary, white Gaussian noise. This process, whose autocorrelation function is an impulse, is self-similar with parameter $H = -1/2$. More typically, though, self-similar processes are nonstationary. For example, the **Wiener process (Brownian motion)** $z(t)$ related to $w(t)$ by[1]

$$z(t) = \int_0^t w(\tau)\, d\tau, \tag{3.3}$$

[1]Throughout this chapter, integrals with respect to the differential element $w(t)\,dt$, where $w(t)$ is a stationary white Gaussian noise, should be interpreted more precisely as integrals with respect to the differential element $dz(t)$, where $z(t)$ is the corresponding Wiener process. While it is customary to consider $w(t)$ to be the derivative of $z(t)$, recall that the nondifferentiability of $z(t)$ means that $w(t)$ is its derivative only in a generalized sense. It is for this reason that an ordinary Riemann integral is technically inadequate, and the

and extended to $t < 0$ through the convention

$$\int_0^t \triangleq -\int_t^0 . \tag{3.4}$$

for all t is statistically self-similar with $H = 1/2$ and nonstationary but, evidently, has a stationary derivative. As a final example, the Gaussian process

$$x(t) = |t|^{H_0 - 1/2} z(t) \tag{3.5}$$

is self-similar with parameter H_0 for all values of H_0, is nonstationary, and has a nonstationary derivative except for $H_0 = 1/2$. In fact, when $x(t)$ in (3.5) is filtered by virtually any nontrivial linear time-invariant filter, the output is a nonstationary process. However, while most physical processes that exhibit self-similarity are fundamentally nonstationary, they retain a stationary quality to them. For this reason, processes such as (3.5) generally constitute rather poor models for such phenomena. By contrast, perhaps the most important class of models for such phenomena are the so-called "$1/f$ processes."

3.2 $1/f$ PROCESSES

The $1/f$ family of statistically self-similar random processes are generally defined as processes having measured power spectra obeying a power law relationship of the form

$$S_x(\omega) \sim \frac{\sigma_x^2}{|\omega|^\gamma} \tag{3.6}$$

for some spectral parameter γ related to H according to

$$\gamma = 2H + 1. \tag{3.7}$$

Generally, the power law relationship (3.6) extends over several decades of frequency. While data length typically limits access to spectral information at lower frequencies, data resolution typically limits access to spectral content at higher frequencies. Nevertheless, there are many examples of phenomena for which arbitrarily large data records justify a $1/f$ spectrum of the form (3.6) over all accessible frequencies. However, (3.6) is not integrable and hence, strictly speaking, does not constitute a valid power spectrum in the theory of stationary random processes. As a consequence, there have been numerous attempts to attach an interpretation to such spectra based on notions of generalized spectra [39] [42] [43] [44].

As a consequence of their inherent self-similarity, the sample paths of $1/f$ processes are typically fractals [4]. In general, the graphs of sample paths

corresponding Riemann-Stieltjes integral is required. Nevertheless, we retain the notation $w(t)\,dt$ for conceptual convenience.

of random processes are one-dimensional curves in the plane. This we refer to as their "topological dimension." However, fractal random processes have sample paths that are so irregular that their graphs have an "effective" dimension that exceeds their topological dimension of unity. It is this effective dimension that is usually referred to as the "fractal" dimension of the graph. However, it is important to note that the notion of fractal dimension is not uniquely defined. There are several different definitions of fractal dimension—each with subtle but important differences—from which to choose for a given application [45]. Nevertheless, regardless of the particular definition, the fractal dimension D of the graph of an ordinary function typically ranges between $D = 1$ and $D = 2$. Larger values of D correspond to functions whose graphs are increasingly rough in appearance and, in an appropriate sense, fill the plane in which the graph resides to a greater extent.

For $1/f$ processes, there is a strong relationship between the fractal dimension D and the self-similarity parameter H of the process. In particular, an increase in the parameter H yields a decrease in the dimension D. This is intuitively reasonable: an increase in H corresponds to an increase in γ, which, in turn, reflects a redistribution of power from high to low frequencies and leads to sample functions that are increasingly smooth in appearance. Fig. 3.1 illustrates some sample paths of $1/f$ processes corresponding to various values of γ. It is worth noting that what we have plotted are, in some sense, bandpass filtered versions of the sample functions, since the finite data length constrains the lowest accessible frequency and the discretization of the time-axis constrains the highest accessible frequency. In Section 3.2.1 we describe the quantitative relationship between a particular notion of fractal dimension D and the self-similarity parameter H for the class of fractional Brownian motion models for $1/f$ processes.

A truly enormous and tremendously varied collection of natural phenomena exhibit $1/f$-type spectral behavior over many decades of frequency. A partial list includes (see, e.g., [4] [43] [46] [47] [48] [49] and the references therein):

- **geophysical time series** such as variation in temperature and rainfall records, measurements of oceanic flows, flood level variation in the Nile river, wobble in the Earth's axis, frequency variation in the Earth's rotation, and sunspot variations;
- **economic time series** such as the Dow Jones Industrial Average;
- **physiological time series** such as instantaneous heart rate records for healthy patients, EEG variations under pleasing stimuli, and insulin uptake rate data for diabetics;
- **biological time series** such as voltages across nerve and synthetic membranes;

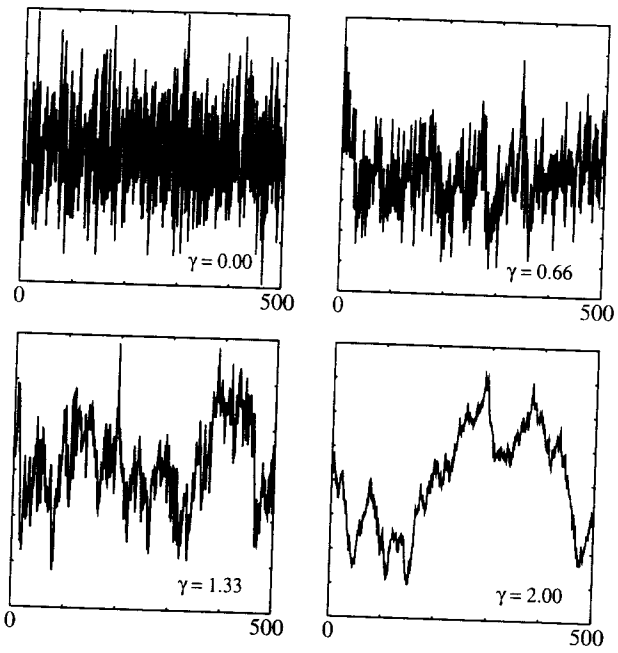

Figure 3.1. Sample paths of $1/f$ processes corresponding to different values of γ.

- **electromagnetic fluctuations** such as in galactic radiation noise, the intensity of light sources, and flux flow in superconductors;
- **electronic device noises** in field effect and bipolar transistors, vacuum tubes, and Schottky, Zener, and tunnel diodes;
- **resistance fluctuations** in metal film, semiconductor films and contacts, germanium filaments in carbon and aqueous solution, thermocells, and concentrations cells;
- **frequency variation** in hourglasses, quartz crystal oscillators, atomic clocks, and superconducting cavity resonators;
- **man-induced phenomena** including variations in traffic flow and amplitude and frequency variation in Western, African, Asian, and Indian music, both modern and traditional;
- **generation of perceptually pleasing physiological stimuli,** such as artificial music and breezes;
- **patterns of burst errors on communication channels;**

- **texture variation in natural terrain,** landscapes, and cloud formations.

While $\gamma \approx 1$ in many of these examples, more generally $0 \leq \gamma \leq 2$. However, there are many examples of phenomena in which γ lies well outside this range. For $\gamma \geq 1$, the lack of integrability of (3.6) in a neighborhood of the spectral origin reflects the preponderance of low-frequency energy in the corresponding processes. This phenomenon is termed **the infrared catastrophe.** For many physical phenomena, measurements corresponding to very small frequencies show no low-frequency roll off, which is usually understood to reveal an inherent nonstationarity in the underlying process. Such is the case for the Wiener process discussed earlier. For $\gamma \leq 1$, the lack of integrability in the tails of the spectrum reflects a preponderance of high-frequency energy and is termed **the ultraviolet catastrophe.** Such behavior is familiar for generalized Gaussian processes such as stationary white Gaussian noise and its usual derivatives.

An important property of $1/f$ processes is their persistent statistical dependence. Indeed, the generalized Fourier pair [50]

$$\frac{|\tau|^{\gamma-1}}{2\Gamma(\gamma)\cos(\gamma\pi/2)} \longleftrightarrow \frac{1}{|\omega|^{\gamma}} \tag{3.8}$$

valid for $\gamma > 0$ but $\gamma \neq 1, 2, 3, \ldots$, suggests that the autocorrelation $R_x(\tau)$ associated with the spectrum (3.6) for $0 < \gamma < 1$ is characterized by slow decay of the form

$$R_x(\tau) \sim |\tau|^{\gamma-1}.$$

This power law decay in correlation structure distinguishes $1/f$ processes from many traditional models for time series analysis. Indeed, the well-studied family of autoregressive moving-average (ARMA) models have a correlation structure invariably characterized by *exponential* decay. As a consequence, ARMA models are generally inadequate for capturing long-term dependence in data.

Perhaps the most important families of $1/f$ processes are those that are non-Gaussian. Indeed, a number of rich and interesting examples of non-Gaussian self-similar behavior can be constructed by exploiting the theory of stable distributions [39] [51] [52] [53]. Nevertheless, Gaussian models are generally applicable in a broad range of contexts, and are analytically highly tractable. For these reasons, we focus principally on Gaussian $1/f$ processes in the sequel.

In the next section, we review what are perhaps the most popular mathematical models for Gaussian $1/f$ processes: **fractional Brownian motion** and **fractional Gaussian noise.** Unavoidably, several mathematical subtleties arise in the development of fractional Brownian motion, making this section somewhat less accessible to the nonspecialist than others. However, while

insightful, a detailed understanding of these subtleties is not essential to appreciating the main results of the chapter. For these reasons, the reader may find it easier to skip over this section on a first reading, proceeding directly to Section 3.2.2. There we develop a powerful but much simpler mathematical characterization for $1/f$ processes.

3.2.1 Fractional Brownian Motion and Fractional Gaussian Noise

It is generally agreed [4] [39] [53] that fractional Brownian motion (fBm) and fractional Gaussian noise (fGn) models were first proposed by Kolmogorov, although their current popularity is undoubtedly due to Mandelbrot who independently derived the theory with Van Ness [39] and promoted their use in numerous subsequent publications (see, e.g., the references in [4]). An extensive bibliographic guide to various subsequent developments of the theory, principally in the mathematics literature, is presented in Taqqu [53].

In this framework, processes corresponding to $1 < \gamma < 3$, for which there is infinite low-frequency power, are developed as nonstationary random processes having finite-power in any finite time interval. These processes are the **fractional Brownian motions**, and classical Brownian motion is a special case corresponding to $\gamma = 2$. By contrast, processes corresponding to $-1 < \gamma < 1$, for which there is infinite high-frequency power, are developed as generalized stationary Gaussian processes corresponding to the derivative of a fractional Brownian motion. These processes are the **fractional Gaussian noises**, and stationary white Gaussian noise is a special case corresponding to $\gamma = 0$. The theory does not directly accommodate the cases $\gamma > 3$ and $\gamma < -1$, although extensions can be formulated. Furthermore, somewhat disturbingly, the models are degenerate for the cases $\gamma = -1$, $\gamma = 1$, and $\gamma = 3$.

To develop the concept, we begin by exploring the possibility of developing $1/f$ models as the result of driving stationary white Gaussian noise through a suitable linear time-invariant system. In this case, a natural choice would be the system with impulse response

$$v(t) = \frac{1}{\Gamma(H+1/2)} t^{H-1/2} u(t), \tag{3.9}$$

where $u(t)$ is the unit-step function

$$u(t) = \begin{cases} 1 & t \geq 0 \\ 0 & t < 0 \end{cases},$$

and where $\Gamma(\cdot)$ is the gamma function. Indeed, (3.9) has the generalized Laplace transform [54]

$$\Upsilon(s) = \frac{1}{s^{H+1/2}},$$

which suggests that if the input $w(t)$ has spectral density σ_x^2, the output will have a power spectrum, in some sense, of the form (3.6) where γ is given via (3.7). As we discuss in Chapter 7, (3.9) represents an example of a linear jointly time- and scale-invariant system of degree $H + 1/2$. However, the system defined via (3.9) is unstable except for the degenerate case $H = -1/2$. Consequently, the convolution

$$x(t) = v(t) * w(t) = \frac{1}{\Gamma(H+1/2)} \int_{-\infty}^{t} (t-\tau)^{H-1/2} w(\tau)\, d\tau \tag{3.10}$$

is not well defined.

In developing their $1/f$ model, Barnes and Allan [55] addressed this dilemma by keying the integration in (3.10) to the time origin, defining their self-similar process by

$$x(t) = \frac{1}{\Gamma(H+1/2)} \int_{0}^{t} |t-\tau|^{H-1/2} w(\tau)\, d\tau \tag{3.11}$$

where this definition is extended for $t < 0$ through the convention (3.4). It is interesting to remark that (3.11) is familiar in mathematics as the **Riemann-Liouville integral** of $w(\tau)$ over the interval $0 < \tau < t$. In fractional calculus theory [56], it often is used to define the fractional integral of $w(t)$ of order $\lambda = H + 1/2 > 0$, usually denoted

$$x(t) = \frac{d^{-\lambda}}{dt^{-\lambda}} w(t).$$

The resulting process is well defined, satisfies $x(0) = 0$, and is statistically self-similar with parameter H, i.e., with $t, s, a > 0$,

$$R_x(t,s) = \sigma_x^2 \int_0^{\min(t,s)} (t-\tau)^{H-1/2} (s-\tau)^{H-1/2}\, d\tau = a^{-2H} R_x(at, as) \tag{3.12}$$

However, the Barnes-Allan process constitutes a rather poor model for $1/f$ behavior. In fact, it lacks any kind of stationary quality. For instance, the increment process

$$\Delta x(t;\varepsilon) \triangleq \frac{x(t+\varepsilon) - x(t)}{\varepsilon} \tag{3.13}$$

while statistically self-similar, satisfying

$$\Delta x(t;\varepsilon) \overset{\mathcal{P}}{=} a^{-(H-1)} \Delta x(at; a\varepsilon) \tag{3.14}$$

for every $\varepsilon > 0$, is nonstationary. Consequently, one cannot associate a stationary generalized derivative with the process. In effect, the underlying problem is that the Barnes-Allan process places too much emphasis on the time origin [39].

Fractional Brownian motion represents a very useful refinement of the Barnes-Allan process. Specifically, fractional Brownian motion is a nonstationary Gaussian self-similar process $x(t)$ also satisfying $x(0) = 0$, but defined

in such a way that its corresponding increment process $\Delta x(t;\varepsilon)$ is self-similar *and* stationary for every $\varepsilon > 0$. Imposing these constraints on increments of fractional Brownian motion leads to a comparatively better model for $1/f$ behavior.

A convenient though specialized definition of fractional Brownian motion is given by Barton and Poor [57]

$$x(t) \triangleq \frac{1}{\Gamma(H+1/2)}\left[\int_{-\infty}^{0}\left(|t-\tau|^{H-1/2}-|\tau|^{H-1/2}\right)w(\tau)\,d\tau + \int_{0}^{t}|t-\tau|^{H-1/2}\,w(\tau)\,d\tau\right] \quad (3.15)$$

for $0 < H < 1$, where $w(t)$ is a zero-mean, stationary white Gaussian noise process with unit spectral density. Again, for $t < 0$, $x(t)$ is defined through the convention (3.4). Note that with $H = 1/2$, (3.15) specializes to the Wiener process (3.3), i.e., classical Brownian motion.

As suggested earlier, fractional Brownian motions are, in fact, fractals. Specifically, it is possible to show (see, e.g., [4] or [45]) that sample functions of fractional Brownian motions whose self-similarity parameters lie in the range $0 < H < 1$ (i.e., $1 < \gamma < 3$) have a fractal dimension (in the Hausdorff-Besicovitch sense) given by

$$D = 2 - H$$

that again gives a quantitative measure of their roughness.

The correlation function for fractional Brownian motion can be readily derived as

$$R_x(t,s) = E[x(t)x(s)] = \frac{\sigma_H^2}{2}\left(|s|^{2H}+|t|^{2H}-|t-s|^{2H}\right) \quad (3.16)$$

where

$$\sigma_H^2 = \mathbf{var}\,x(1) = \Gamma(1-2H)\frac{\cos(\pi H)}{\pi H}, \quad (3.17)$$

from which it is straightforward to verify that the process is statistically self-similar with parameter H.

It is likewise straightforward to verify that the normalized increments of fractional Brownian motion are stationary and self-similar, and have the autocorrelation

$$R_{\Delta x}(\tau;\varepsilon) \triangleq E[\Delta x(t;\varepsilon)\Delta x(t-\tau;\varepsilon)] = \frac{\sigma_H^2\varepsilon^{2H-2}}{2}\left[\left(\frac{|\tau|}{\varepsilon}+1\right)^{2H}-2\left(\frac{|\tau|}{\varepsilon}\right)^{2H}+\left(\frac{|\tau|}{\varepsilon}-1\right)^{2H}\right]. \quad (3.18)$$

At large lags ($|\tau| \gg \varepsilon$), the correlation is asymptotically given by

$$R_{\Delta x}(\tau) \approx \sigma_H^2 H(2H-1)|\tau|^{2H-2}. \quad (3.19)$$

Letting $\varepsilon \to 0$, and defining

$$H' = H - 1, \quad (3.20)$$

we can reason from (3.15) that fractional Brownian motion has the generalized derivative [57]

$$x'(t) = \frac{d}{dt}x(t) = \lim_{\varepsilon\to 0}\Delta x(t;\varepsilon) = \frac{1}{\Gamma(H'+1/2)}\int_{-\infty}^{t}|t-\tau|^{H'-1/2}\,w(\tau)\,d\tau \quad (3.21)$$

which is termed **fractional Gaussian noise**. Note that (3.21) is precisely a convolution of the form (3.10), for which we now have an interpretation. Furthermore, from this observation we deduce that the derivative process $x'(t)$ is stationary and statistically self-similar with parameter H'.

From (3.18) it is apparent that the character of $x'(t)$ depends strongly on the value of H. Note that the right side of (3.19) has the same algebraic sign as $H - 1/2$. Hence, for $1/2 < H < 1$ this derivative process exhibits long-term dependence, i.e., persistent correlation structure. For $H = 1/2$, this derivative is the usual stationary white Gaussian noise, which has no correlation, while for $0 < H < 1/2$, the derivative exhibits persistent anti-correlation. For $1/2 < H < 1$, $x'(t)$ is zero-mean and stationary with covariance

$$R_{x'}(\tau) = E[x'(t)x'(t-\tau)] = \sigma_H^2(H'+1)(2H'+1)|\tau|^{2H'} \quad (3.22)$$

and we note that the generalized Fourier pair (3.8) suggests that the corresponding power spectral density of the derivative process can be expressed, for $\omega \neq 0$, as

$$S_{x'}(\omega) = \frac{1}{|\omega|^{\gamma'}}, \quad (3.23)$$

where

$$\gamma' = 2H' + 1.$$

The preceding development suggests the conceptually useful synthesis for fractional Brownian motion depicted in Fig. 3.2. In particular, driving a linear time-invariant system with impulse response

$$v(t) = \frac{1}{\Gamma(H-1/2)}t^{H-3/2}u(t)$$

with stationary white Gaussian noise $w(t)$ generates a fractional Gaussian noise $x'(t)$, from which fractional Brownian motion $x(t)$ is obtained by routine integration:

$$x(t) = \int_0^t x'(t)\,dt.$$

The fractional Brownian motion framework provides a useful construction for some models of $1/f$-type spectral behavior corresponding to spectral

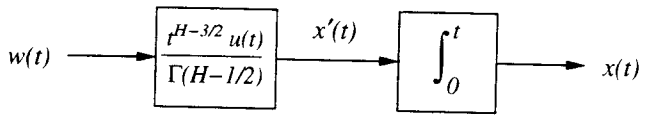

Figure 3.2. Synthesis of fractional Brownian motion $x(t)$ in terms of fractional Gaussian noise $x'(t)$ and stationary white Gaussian noise $w(t)$.

exponents in the range $-1 < \gamma < 1$ and $1 < \gamma < 3$. In fact, they uniquely model certain classes of $1/f$ behavior. One can show, for instance, that for $0 < H < 1$, fractional Brownian motion constitutes the *only* statistically self-similar, zero-mean, mean-square continuous, finite-variance, Gaussian random process satisfying $x(0) = 0$ and having stationary increments. While these are somewhat restrictive conditions, this framework has, in general, become a popular one for modeling a variety of phenomena with $1/f$ behavior (see, e.g., [4] [47] [57] [58]). However, fractional Brownian motion and fractional Gaussian noise are not the only models for $1/f$ behavior, even within the respective parameter ranges $-1 < \gamma < 1$ and $1 < \gamma < 3$. In fact, in some cases they constitute rather poor models for $1/f$ behavior.

One unsatisfying characteristic of fractional Brownian motion is its pronounced time origin. Indeed, fractional Brownian motion satisfies not only $x(0) = 0$, but also power law growth in variance as a function of time, i.e.,

$$\operatorname{var} x(t) = \sigma_H^2 |t|^{2H}.$$

In modeling many physical phenomena having empirical spectra corresponding to γ in this range, the notion of such a time origin is not only rarely observed, but rather unnatural as well.

Additionally, the fractional Brownian motion framework has a number of limitations. In particular, it does not lead to useful models for $1/f$ processes corresponding to $\gamma \leq -1$, $\gamma \geq 3$, and perhaps the most important and ubiquitous case, $\gamma = 1$. Indeed, for $\gamma = 3$ ($H = 1$), fractional Brownian motion as defined by (3.15) degenerates to a process whose sample paths are all lines through the origin, viz.,

$$x(t) = |t|x(1).$$

For $\gamma = 1$ ($H = 0$), fractional Brownian motion degenerates to the trivial process

$$x(t) \equiv 0.$$

More generally, choosing $H < 0$ in (3.15) leads to processes that are not continuous (in the mean-square sense), while choosing $H > 1$ in (3.15) leads to processes whose increments (and, hence, generalized derivatives) are not stationary [39] [52].

In the next section, we consider a more general but nonconstructive model for $1/f$ processes that includes both fractional Brownian motions and fractional Gaussian noises, yet appears to avoid some of the restrictions imposed by the fractional Brownian motion framework. This mathematical characterization for $1/f$ processes was originally developed in Wornell [59] [60].

3.2.2 A Mathematical Characterization in the Frequency Domain

The notion that measurements of spectra for physical processes can only be obtained over a range of frequencies governed by data length and resolution limitations suggests a potentially useful approach for *defining* $1/f$ processes. In particular, let us consider defining $1/f$ processes in terms of their characteristics under bandpass filtering specifically as follows.

Definition 3.1 *A wide-sense statistically self-similar zero-mean random process $x(t)$ is said to be a* $1/f$ process *if there exist ω_0 and ω_1 satisfying $0 < \omega_0 < \omega_1 < \infty$ such that when $x(t)$ is filtered by an ideal bandpass filter with frequency response*

$$B_1(\omega) = \begin{cases} 1 & \omega_0 < |\omega| \leq \omega_1 \\ 0 & \text{otherwise} \end{cases} \tag{3.24}$$

the resulting process $y_1(t)$ is wide-sense stationary and has finite variance.

Before exploring the implications and insights that arise from this definition, it is useful to point out that choosing an ideal bandpass filter in this definition may, in fact, not be critical. It might suffice, for example, to choose any filter whose frequency response $B(\omega)$ has sufficient decay as $\omega \to 0$ and $\omega \to \infty$. Whether this leads to an equivalent definition remains an open question. Nevertheless, the use of ideal filters is certainly rather convenient. Indeed, the fundamental appeal of Definition 3.1 as a characterization for $1/f$ processes is its basis in the frequency-domain. As a consequence, this allows us to extend the well-established tools of Fourier analysis to this important class of nonstationary processes. In turn, we are able to derive a number of new properties of $1/f$ processes in a highly efficient manner.

The following theorem justifies designating processes satisfying Definition 3.1 as $1/f$ processes, and leads to an important interpretation of the spectrum (3.6) for these processes. A detailed but straightforward proof is provided in Appendix B.1.

Theorem 3.2 *A $1/f$ process $x(t)$, when filtered by an ideal bandpass filter with frequency response*

$$B(\omega) = \begin{cases} 1 & \omega_L < |\omega| \leq \omega_U \\ 0 & \text{otherwise} \end{cases} \tag{3.25}$$

for arbitrary $0 < \omega_L < \omega_U < \infty$, yields a wide-sense stationary random process $y(t)$ with finite variance and having power spectrum

$$S_y(\omega) = \begin{cases} \sigma_x^2/|\omega|^\gamma & \omega_L < |\omega| \le \omega_U \\ 0 & \text{otherwise} \end{cases} \tag{3.26}$$

for some $\sigma_x^2 > 0$, and where the spectral exponent γ is related to the self-similarity parameter H according to $\gamma = 2H + 1$.

Of course, an important question that must be addressed concerns whether there exist any nontrivial random processes satisfying Definition 3.1. Fortunately, the answer is yes, and the following theorem constitutes an existence proof, verifying that Definition 3.1 is nondegenerate for at least some values of γ. In particular, the theorem establishes that it is possible to construct families of Gaussian processes that satisfy this definition. A straightforward proof is provided in Appendix B.2.

Theorem 3.3 *Fractional Brownian motions corresponding to $0 < H < 1$ and the associated fractional Gaussian noises are $1/f$ processes in the sense of Definition 3.1.*

We remark that, based on our discussion of Section 3.2.1, an immediate corollary is that the Wiener process and stationary white Gaussian noise are also $1/f$ processes. In contrast, the Barnes-Allan process we described at the outset of Section 3.2.1 is not a $1/f$ process in the sense of Definition 3.1. This is to be expected, given the shortcomings of the Barnes-Allan process in modeling $1/f$-type behavior.

Another question that naturally arises concerns whether there are any other Gaussian $1/f$ processes besides those of Theorem 3.3. For instance, is it possible to construct nontrivial Gaussian processes that satisfy Definition 3.1 for values of H outside $0 < H < 1$? And, are there other Gaussian processes satisfying this definition for $0 < H < 1$? Recent work [61] indirectly suggests that the answer to this last question may be negative, although such a result is not explicitly proved. In effect, this paper shows that if we were to replace the bandpass filter (3.24) in Definition 3.1 with a roughly bandpass filter whose frequency response is differentiable, has a simple zero at $\omega = 0$, and decays sufficiently quickly as $\omega \to \infty$, then the definition uniquely characterizes fractional Brownian motion. However, the constraints on the filter they consider are overly restrictive to answer our specific questions. Furthermore, it may be that the technical definition of a random process they consider is too narrowly chosen to accommodate $1/f$ behavior.

In any event, a practical difficulty with both the fractional Brownian motion framework and the frequency-based characterization for $1/f$ processes just described is that while mathematically well defined, neither is analytically convenient in many contexts. In fact, there are many very basic signal processing problems that are effectively intractable using these models.

To address this limitation, we next consider some more general classes of *$1/f$-like* models. While these models typically do not give rise to *exactly-$1/f$* spectra, they give rise to spectra that are *nearly-$1/f$*. As we will see, many of these processes retain most of the fundamental characteristics of $1/f$ processes, yet are considerably more amenable to analysis.

3.3 NEARLY-$1/f$ PROCESSES

Perhaps the best-known class of nearly-$1/f$ processes have been those based upon a generalized, infinite-order autoregressive moving-average (ARMA) framework. We review two such formulations before developing a wavelet-based model for $1/f$-type behavior that is the focus of the chapter.

3.3.1 ARMA Models

There have been a variety of attempts to exploit a generalized autoregressive moving-average framework in modeling $1/f$ processes. Perhaps the earliest such framework, based on a "distribution of time constants" formulation, arose in the physics literature and dates back at least to the work of Bernamont [62]. However, it was really the seminal paper of van der Ziel [63] that sparked substantial interest in this approach, and much subsequent development.

Van der Ziel's basic approach was to model a $1/f$ process as the weighted superposition of an infinite number of uncorrelated random processes, each governed by a distinct characteristic time-constant $1/\alpha > 0$. Each of these random processes has correlation function

$$R_\alpha(\tau) = e^{-\alpha|\tau|}$$

corresponding to a Lorenzian spectra of the form

$$S_\alpha(\omega) = \frac{2\alpha}{\alpha^2 + \omega^2}$$

and can be modeled as the output of a causal LTI filter with system function

$$\Upsilon_\alpha(s) = \frac{\sqrt{2\alpha}}{s + \alpha}$$

driven by an independent stationary white noise source. The weighted superposition of a continuum of such processes has an effective spectrum

$$S_x(\omega) = \int_0^\infty S_\alpha(\omega)\, f(\alpha)\, d\alpha \tag{3.27}$$

where the weights $f(\alpha)$ correspond to the density of poles or, equivalently, relaxation times. If an unnormalizable, scale-invariant density of the form

$$f(\alpha) = \alpha^{-\gamma} \tag{3.28}$$

for $0 < \gamma < 2$ is chosen, the resulting spectrum (3.27) is $1/f$, i.e.,

$$S_x(\omega) \propto \frac{1}{|\omega|^\gamma}.$$

This mathematical identity suggests a useful and practical approach to modeling $1/f$-type behavior using the superposition of a *countable* collection of single time-constant processes whose poles are appropriately distributed. In fact, the density (3.28) implies that the poles should be uniformly distributed along a logarithmic frequency axis. The resulting process $x(t)$ synthesized in this manner then has a nearly-$1/f$ spectrum in the following sense: when $x(t)$ is filtered by any bandpass filter of the form (3.25) the result is a stationary process whose spectrum within the passband is $1/f$ with superimposed ripple that is uniform-spaced and of uniform amplitude on a log-log frequency plot.

As an example, consider exponentially spaced poles according to

$$\alpha_m = \Delta^m, \qquad -\infty < m < \infty, \tag{3.29}$$

for some $1 < \Delta < \infty$. Then the limiting spectrum

$$S_x(\omega) = \sum_m \frac{\Delta^{(2-\gamma)m}}{\omega^2 + \Delta^{2m}} \tag{3.30}$$

is bounded according to

$$\frac{\sigma_L^2}{|\omega|^\gamma} \le S_x(\omega) \le \frac{\sigma_U^2}{|\omega|^\gamma} \tag{3.31}$$

for some $0 < \sigma_L^2 \le \sigma_U^2 < \infty$, and has ripple such that for all integers k

$$|\omega|^\gamma S_x(\omega) = |\Delta^k \omega|^\gamma S_x(\Delta^k \omega). \tag{3.32}$$

As Δ is chosen closer to unity, the pole spacing decreases, which results in a decrease in both the amplitude and spacing of the spectral ripple on a log-log plot.

Note that we may interpret the $1/f$ model that results from this discretization as an infinite-order ARMA process. That is, $x(t)$ can be viewed as the output of a rational LTI system with a countably infinite number of both poles and zeros driven by a stationary white noise source. There has been a substantial body of literature that has attempted to exploit this distribution-of-time-constants model in an effort to explain the ubiquity of $1/f$ spectra in nature. In essence, studies [64] [65] [66] construct mathematical arguments to the effect that $1/f$ spectra are the result of large, complex systems in nature favoring scale-invariant time-constant distributions of the form (3.28).

Somewhat more recently, Keshner [43] [46] developed an alternative ARMA-based model for $1/f$-like behavior from an engineering perspective.

This approach, which has also received considerable attention in the literature, is based on the observation that an infinite-length continuous RC transmission line when driven with a stationary white noise current $i(t)$ yields a measured voltage $v(t)$ whose power spectrum is of the form (3.6) for $0 < \gamma < 2$. That is, in some sense, the impedance function of the line is of the form

$$\frac{V(s)}{I(s)} \propto \frac{1}{s^{\gamma/2}}.$$

By considering an infinite-length, *lumped*-parameter RC line as an approximation, Keshner showed that this gave rise to nearly-$1/f$ behavior in much the same manner as was obtained in the van der Ziel model. It is possible to interpret $1/f$ processes obtained in this manner as the result of driving stationary white noise through an LTI system with a rational system function

$$\Upsilon(s) = \prod_{m=-\infty}^{\infty} \left[\frac{s + \Delta^{m+\gamma/2}}{s + \Delta^m} \right] \tag{3.33}$$

which, in turn, leads to a spectrum of the form

$$S_x(\omega) \propto \prod_{m=-\infty}^{\infty} \left[\frac{\omega^2 + \Delta^{2m+\gamma}}{\omega^2 + \Delta^{2m}} \right]. \tag{3.34}$$

This nearly-$1/f$ spectrum has the same properties as the van der Ziel spectrum, satisfying both (3.31) and (3.32). In fact, comparing the spectra (3.34) and (3.30), we see that the pole placement strategy for both is identical. However, the zeros in the two models are, in general, distributed much differently. This, in turn, leads to differing degrees of ripple amplitude for a given pole spacing for the two different models [67].

It is interesting to remark that the idea of using infinite lumped RC line to realize such systems was independently developed in the context of fractional calculus. Indeed, Oldham and Spanier [56] describe precisely such an implementation for fractional integration operators of the type used in the construction of the Barnes-Allan process (3.11).

The structure of the system function (3.33) of Keshner's synthesis filter provides additional insights into $1/f$-like behavior. For example, the infinity of poles suggests that a state space characterization of $1/f$ processes would generally require uncountably many state variables, consistent with the notion of long-term correlation structure in such processes.

Also, this system function lends useful insight into the limiting behavior of $1/f$ processes as $\gamma \to 0$ and $\gamma \to 2$. Note that the poles and zeros of (3.33) lie along the negative real axis in the s-plane. On a logarithmic scale, the poles and zeros are each spaced uniformly along this half-line. Furthermore, in general, to the left of each pole in the s-plane lies a matching zero, so that poles and zeros are alternating along the half-line. However, for certain

values of γ, pole-zero cancellation takes place. In particular, as $\gamma \to 2$, the zero pattern shifts left canceling all poles except the limiting pole at $s = 0$. The resulting system is therefore an integrator, characterized by a single state variable, and generates a Wiener process as anticipated. By contrast, as $\gamma \to 0$, the zero pattern shifts right canceling all poles. The resulting system is therefore a multiple of the identity system, requires no state variables, and generates stationary white noise as anticipated.

Finally, note that the model may be interpreted in terms of a Bode plot. In general, stable, rational system functions comprised of real poles and zeros are only capable of generating transfer functions whose Bode plots have slopes that are integer multiples of

$$20 \log_{10} 2 \approx 6 \qquad \text{dB/octave.}$$

However, a $1/f$ synthesis filter must fall off at

$$10\gamma \log_{10} 2 \approx 3\gamma \qquad \text{dB/octave}$$

where $0 < \gamma < 2$ is generally not an integer.[2] To accommodate such slopes using rational system functions requires an alternating sequence of poles and zeros to generate a stepped approximation to a -3γ dB/octave slope from segments that alternate between slopes of -6 dB/octave and 0 dB/octave.

Unfortunately, neither of the ARMA-based models have been particularly useful in addressing basic problems of detection and estimation involving $1/f$ processes. However, both have been used extensively as $1/f$ noise simulators. A discrete-time implementation of the van der Ziel model is described by Pellegrini et al. [68], while details of a discrete-time implementation of Keshner's model appears in Corsini and Saletti [69]. A comparison of the two approaches is presented in Saletti [67]. In virtually all the simulations we present, the Corsini-Saletti implementation of Keshner's model is used to synthesize $1/f$ processes. In particular, the $1/f$ sample paths of Fig. 3.1 are obtained via this algorithm.

3.3.2 Wavelet-Based Models

In this section, we explore the relationship between orthonormal wavelet bases and nearly-$1/f$ models. In particular, we show that wavelet basis expansions are both natural and convenient representations for processes exhibiting $1/f$-like behavior. Our main result is that orthonormal wavelet basis expansions play the role of Karhunen-Loève-type expansions for $1/f$-type processes [59] [60]. That is, wavelet basis expansions in terms of uncorrelated random variables constitute very good models for $1/f$-type behavior.

[2]Noise that falls off at 3dB/octave, which corresponds to $\gamma = 1$, is often referred to as "pink" noise. It arises in a variety of applications. For example, in professional audio systems, room equalization is often performed with a pink noise source.

Synthesis

In this section, we demonstrate that nearly-$1/f$ behavior may be generated from orthonormal wavelet basis expansions in terms of a collections of uncorrelated wavelet coefficients. In particular, we establish the following theorem, an earlier version of which appears in Wornell [70], and whose proof is provided in Appendix B.3.

Theorem 3.4 *Consider any orthonormal wavelet basis with Rth-order regularity for some $R \geq 1$. Then the random process constructed via the expansion*

$$x(t) = \sum_m \sum_n x_n^m \psi_n^m(t), \tag{3.35}$$

where the x_n^m are a collection of mutually uncorrelated, zero-mean random variables with variances

$$\operatorname{var} x_n^m = \sigma^2 2^{-\gamma m}$$

for some parameter $0 < \gamma < 2R$, has a time-averaged spectrum

$$S_x(\omega) = \sigma^2 \sum_m 2^{-\gamma m} |\Psi(2^{-m}\omega)|^2 \tag{3.36}$$

that is nearly-$1/f$, i.e.,

$$\frac{\sigma_L^2}{|\omega|^\gamma} \leq S_x(\omega) \leq \frac{\sigma_U^2}{|\omega|^\gamma} \tag{3.37}$$

for some $0 < \sigma_L^2 \leq \sigma_U^2 < \infty$, and has octave-spaced ripple, i.e., for any integer k

$$|\omega|^\gamma S_x(\omega) = |2^k\omega|^\gamma S_x(2^k\omega). \tag{3.38}$$

In Fig. 3.3 we illustrate the time-averaged spectrum of a process constructed in the manner of this theorem for $\gamma = 1$ using the first order Battle-Lemarie wavelet basis. Note the characteristic octave-spaced ripple. The bounding constants in this case correspond to $\sigma_U^2/\sigma_L^2 = 1.103$.

The result established by this theorem is certainly an intuitively reasonable one if, for example, we view the orthonormal wavelet decomposition as a generalized octave-band filter bank as described in Section 2.3.1. In fact, for the case of the ideal bandpass wavelet basis, it can be readily established from simple geometric arguments that the tightest bounding constants are

$$\begin{aligned} \sigma_L^2 &= \sigma^2 \pi^\gamma \\ \sigma_U^2 &= \sigma^2 (2\pi)^\gamma. \end{aligned}$$

Note, too, the special interpretation that may be derived from the model for the case $\gamma = 1$, arguably the most prevalent of the $1/f$-type processes. Here the choice of the variance progression

$$\operatorname{var} x_n^m = \sigma^2 2^{-m}$$

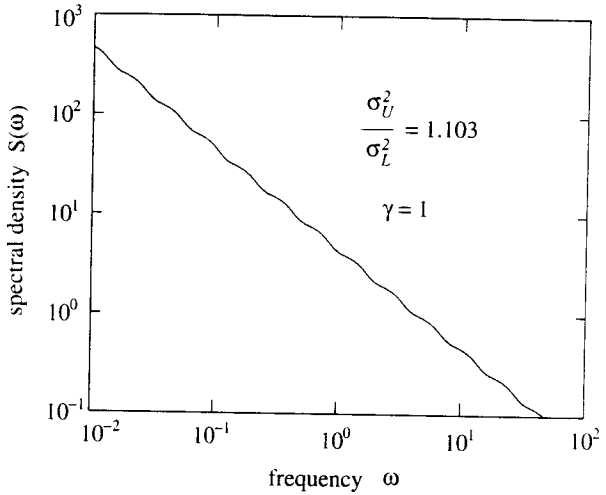

Figure 3.3. The time-averaged spectrum of a process synthesized from the first-order Battle-Lemarie orthonormal wavelet basis. The parameters of the nearly-$1/f$ spectrum are $\gamma = 1$ and $\sigma_U^2/\sigma_L^2 = 1.103$ in this case.

corresponds to distributing power equally among the detail signals at all resolution scales, since we have for each m

$$\frac{1}{2\pi}\int_{-\infty}^{\infty} P_m(\omega)|\Psi(2^{-m}\omega)|^2 d\omega = 1. \tag{3.39}$$

There are two aspects of this theorem that warrant further discussion. First, the nearly-$1/f$ spectrum (3.36) is to be interpreted in the same manner that the $1/f$ spectrum (3.6) is for exactly-$1/f$ processes. That is, if $x(t)$ is filtered by an ideal bandpass filter with frequency response of the form (3.25), the output of the filter will have finite-power and correspond to a spectrum of the form (3.36) over the passband $\omega_L < |\omega| \leq \omega_U$. However, it is important to emphasize that this spectrum is a *time-averaged* one. Indeed, the output of such a bandpass filter will *not*, in general, be stationary in any sense, which is a consequence of the discrete nature of the synthesis. This behavior is in contrast to the ARMA-based nearly-$1/f$ processes discussed in Section 3.3.1, which, when bandpass filtered, yield *stationary* processes with nearly-$1/f$ spectra.

One approach to extending this model so as to incorporate this property of stationarity is to add phase jitter in the synthesis process. Specifically, we may consider randomizing the time-origin of our processes generated via (3.35) by applying a random (positive or negative) delay to the process. In

fact, this is one way of interpreting (3.36) as the generalized spectrum of a stationary process. However, the random process $\check{x}(t)$ constructed in this way is no longer ergodic. Furthermore, if the coefficients x_n^m in Theorem 3.4 are chosen to be Gaussian, $x(t)$ will be necessarily a Gaussian process, but $\check{x}(t)$ will not. For these reasons, the phase-jittered process, while perhaps useful for synthesizing $1/f$-like behavior, is difficult to exploit in analyzing $1/f$-like behavior.

Some remarks concerning the conditions on the wavelet basis are also appropriate. We begin by noting that to generate $1/f$-like behavior for $0 < \gamma < 2$, it suffices to use a wavelet basis for which the corresponding multiresolution analysis is at least *regular*. Again, virtually any practical wavelet basis satisfies this condition, even the Haar basis. However, the theorem implies that to generate $1/f$-like behavior for $\gamma > 2$, higher regularity ($R > 1$) is required. This can be verified experimentally as well. We find, for instance, that when we attempt to synthesize $1/f$-like behavior for $\gamma = 5$ using bases with $R \geq 3$, the sample functions are characterized by a smoothness consistent with the decay in their spectra. However, when bases corresponding to $R < 3$ are used in the synthesis, the sample functions lose their characteristic smoothness. Specifically, using a Haar-based synthesis ($R = 1$), the sample functions exhibit abrupt discontinuities, while using a second-order ($R = 2$) Daubechies basis leads to sample functions exhibiting abrupt discontinuities in their derivatives. In effect, unless there is sufficient regularity, the characteristics of the basis functions manifest themselves in the sample functions generated by the expansion. However, at least in this context, there would appear to be no benefit to using bases that have more regularity than required by the theorem.

We also remark that a much stronger theorem holds for the case $\gamma = 0$ in which the coefficients are not only uncorrelated but have identical variances. In this case, constructing an expansion from such a collection of random variables in *any* orthonormal basis yields stationary white noise whose spectral density is the variance of the coefficients. In particular, for any wavelet basis we have

$$S_x(\omega) = \sigma^2 = \sigma^2 \sum_m |\Psi(2^{-m})|^2$$

when $\gamma = 0$ where the last equality is a restatement of the identity (2.9) and demonstrates the consistency of this case with (3.36).

Finally, we remark that Theorem 3.4 may, in principle, be extended to $\gamma < 0$ provided the wavelet basis used in the synthesis has a sufficient number of vanishing moments. This can be deduced from the proof in Appendix B.3. However, we do not discuss this extension to the theorem primarily because there would appear to be relatively few, if any, physical processes of interest corresponding to negative γ.

Analysis

In this section, we derive a collection of complementary results to suggest that wavelet bases are equally useful in the analysis of $1/f$ processes. In particular, we provide both theoretical and empirical evidence suggesting that when $1/f$-like processes are expanded in terms of orthonormal wavelet bases, the resulting wavelet coefficients are typically rather weakly correlated, particularly in contrast to the rather strong correlation present in the original process. These results, combined with those of the last section, provide evidence of that such wavelet-based representations are robust characterizations of $1/f$-like behavior with Karhunen-Loève-type properties.

Virtually all the results we obtain in this section are derived conveniently and efficiently in the frequency-domain. In anticipation of these derivations, we first establish the following theorem, whose proof is outlined in Appendix B.4.

Theorem 3.5 *Let $x(t)$ be a $1/f$ process whose spectral parameters, in the sense of Theorem 3.2, are σ_x^2 and $\gamma > 0$. Furthermore, let the wavelet coefficients x_n^m be the projections of $x(t)$ onto some orthonormal wavelet basis. Then the correlation between an arbitrary pair of such coefficients x_n^m and $x_{n'}^{m'}$ is given by*

$$E\left[x_n^m x_{n'}^{m'}\right] = \frac{2^{-(m+m')/2}}{2\pi}\int_{-\infty}^{\infty}\frac{\sigma_x^2}{|\omega|^\gamma}\,\Psi(2^{-m}\omega)\,\Psi^*(2^{-m'}\omega)\,e^{-j\left(n2^{-m}-n'2^{-m'}\right)\omega}\,d\omega \tag{3.40}$$

for any choice of $\psi(t)$ and γ such that this integral is convergent.

The principal shortcoming of this theorem is that it fails to establish conditions on the wavelet basis and γ under which (3.40) is defined. Nevertheless, we may generally use Theorem 3.5 to derive properties of the second-order statistics of wavelet coefficients of $1/f$ processes for $\gamma > 0$. For instance, an immediate consequence of the theorem is that we can show the variance of the x_n^m to be of the form

$$\operatorname{var} x_n^m = \sigma^2 2^{-\gamma m}$$

where

$$\sigma^2 = \frac{1}{2\pi}\int_{-\infty}^{\infty}\frac{\sigma_x^2}{|\omega|^\gamma}\,|\Psi(\omega)|^2\,d\omega.$$

To obtain this result, it suffices to let $m' = m$ and $n' = n$ in (3.40) and effect a change of variables.

Defining

$$\rho_{n,n'}^{m,m'} \triangleq \frac{E\left[x_n^m x_{n'}^{m'}\right]}{\sqrt{(\operatorname{var} x_n^m)(\operatorname{var} x_{n'}^{m'})}} \tag{3.41}$$

as the *normalized* wavelet correlation, a second consequence is that the wavelet coefficients are wide-sense stationary at each scale, i.e., for a fixed scale m, $\rho_{n,n'}^{m,m}$ is a function only of $n - n'$. Specifically, we may readily establish that

$$\rho_{n,n'}^{m,m} = \frac{1}{2\pi\sigma^2}\int_{-\infty}^{\infty}\frac{\sigma_x^2}{|\omega|^\gamma}\,|\Psi(\omega)|^2\,e^{-j(n-n')\omega}\,d\omega. \tag{3.42}$$

Again, this result may be obtained by specializing (3.40) to the case $m' = m$ and effecting a change of variables.

We can also show that the normalized wavelet coefficients possess a kind of stationarity *across* scales as well. Recalling from Section 2.3.1 the critically sampled filter bank interpretation of the wavelet decomposition, whereby the output of the mth filter was sampled at rate $t = 2^{-m}n$ for $n = \ldots, -1, 0, 1, 2, \ldots$, we note that a pair of wavelet coefficients x_n^m and $x_{n'}^{m'}$ at distinct scales m and m' correspond to synchronous time-instants precisely when

$$2^{-m}n = 2^{-m'}n'. \tag{3.43}$$

Our stationarity result in this case is that the normalized correlation among time-synchronous wavelet coefficients corresponding to scales m and m' is a function only of $m - m'$. More precisely, we can show that whenever (3.43) holds,

$$\rho_{n,n'}^{m,m'} = \frac{1}{2\pi\sigma^2}2^{-(m-m')/2}\int_{-\infty}^{\infty}\frac{\sigma_x^2}{|\omega|^\gamma}\,\Psi(2^{-(m-m')}\omega)\,\Psi^*(\omega)\,d\omega. \tag{3.44}$$

Again, this result follows from specializing (3.40) and effecting a change of variables.

The above results verify that the wavelet coefficients of $1/f$ processes obey the variance progression anticipated from the synthesis result. Moreover, the stationarity results provide insight into the correlation structure among wavelet coefficients. However, what we seek ideally are good bounds on the magnitude of the correlation among wavelet coefficients both in the case that they reside at the same scale, and in the case they reside at distinct scales. Certainly, as we will see, there is strong empirical evidence that the correlation among coefficients is rather small and, in most cases, negligible. The following theorem provides some theoretical evidence by establishing an asymptotic result. A proof is provided in Appendix B.5.

Theorem 3.6 *Consider an orthonormal wavelet basis such that $\psi(t)$ has R vanishing moments, i.e.,*

$$\Psi^{(r)}(\omega) = 0, \qquad r = 0, 1, \cdots, R-1 \tag{3.45}$$

for some integer $R \geq 1$. Then provided $0 < \gamma < 2R$, the wavelet coefficients obtained by projecting a $1/f$ process onto this basis have a correlation whose magnitude decays

according to[3]

$$|\rho_{n,n'}^{m,m'}| \sim \mathcal{O}\left(|2^{-m}n - 2^{-m'}n'|^{-\lceil 2R-\gamma \rceil}\right) \tag{3.46}$$

as

$$|2^{-m}n - 2^{-m'}n'| \to \infty.$$

While this theorem makes an interesting statement about the *relative* correlation among some wavelet coefficients well-separated in (m, n)-space, we must avoid inferring some stronger statements. First, it says nothing about the correlation among time-synchronous wavelet coefficients [i.e., those satisfying (3.43)], regardless of how well-separated they are. Furthermore, while plausible, the theorem itself does not assert that choosing an analysis wavelet with a larger number of vanishing moments can reduce the correlation among wavelet coefficients in the analysis of $1/f$ processes. Likewise, the theorem does not actually validate the reasonable hypothesis that choosing a wavelet with an insufficient number of vanishing moments leads to strong correlation among the wavelet coefficients of $1/f$ processes. In fact, the theorem identifies neither a range of m, m', n, n' over which (3.46) holds, nor a leading multiplicative constant in (3.46). Consequently, this precludes us from inferring anything about the *absolute* correlation between *any* particular pair of coefficients.

For the case of the ideal bandpass wavelet basis, however, we may obtain some more useful bounds on the correlation among wavelet coefficients. In this case, the basis functions corresponding to distinct scales have non-overlapping frequency support. Hence, carefully exploiting the stationarity properties of $1/f$ processes developed in Theorem 3.2, we conclude that the wavelet coefficients corresponding to distinct scales are uncorrelated, However, at a given scale the correlation at integral lag $l \geq 0$ is non-zero and may be expressed as

$$\rho_{n,n-l}^{m,m} = \frac{\sigma_x^2}{\pi\sigma^2} \int_{\pi}^{2\pi} \omega^{-\gamma} \cos(\omega l)\, d\omega \tag{3.47}$$

where

$$\frac{\sigma^2}{\sigma_x^2} = \begin{cases} (2^{1-\gamma} - 1)/(\pi^{\gamma}(1-\gamma)) & \gamma \neq 1 \\ (\ln 2)/(\pi) & \gamma = 1 \end{cases}. \tag{3.48}$$

While (3.47) cannot be evaluated in closed form, integrating by parts twice and using the triangle inequality gives the useful closed-form bound

$$|\rho_{n,n-l}^{m,m}| \leq \frac{\sigma_x^2}{\sigma^2} \frac{\gamma}{l^2\pi^{2+\gamma}} \left\{ 1 + \frac{1}{2^{1+\gamma}} + \frac{1+\gamma}{l\pi} \left[1 - \frac{1}{2^{2+\gamma}} \right] \right\} \tag{3.49}$$

valid for $\gamma \geq 0$ and integer-valued $l \geq 1$.

[3]The ceiling function $\lceil x \rceil$ denotes the smallest integer greater than or equal to x.

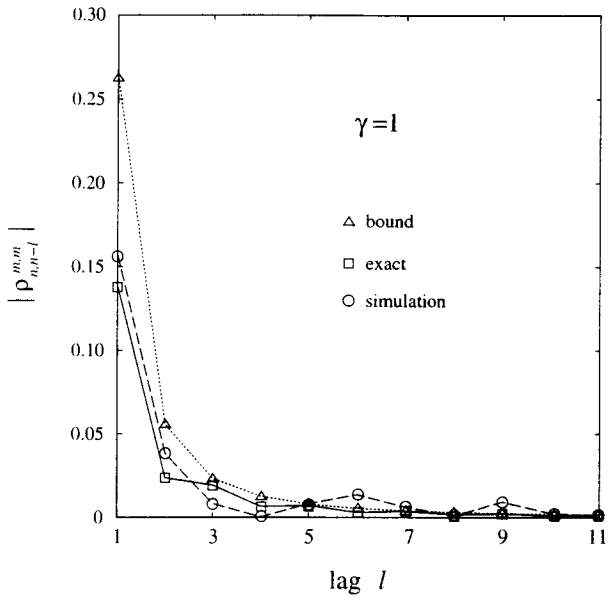

Figure 3.4. Along-scale correlation between wavelet coefficients for an exactly-$1/f$ process for which $\gamma = 1$. The squares □ indicate a numerical estimate of the exact magnitude of the normalized correlation between wavelet coefficients as a function of the lag l between them. The ideal bandpass wavelet was assumed in the analysis. The triangles △ indicate the corresponding values of the closed-form bound obtained in the text. The circles ○ show the average sample-correlation as computed from projections of a $1/f$ process generated using Keshner's synthesis onto a 5th-order Daubechies wavelet basis.

In Fig. 3.4, we plot the exact magnitude of the normalized correlation (3.47) obtained by numerical integration as a function of lag l together with the bound (3.49). Note that correlation among wavelet coefficients is extremely small: adjacent coefficients have a correlation coefficient of less than 15 percent, and more widely separated coefficients have a correlation coefficient less than 3 percent. Hence, it is not an unreasonable approximation to neglect the intercoefficient correlation in any analysis using this wavelet basis.

On the same plot we superimpose the average along-scale sample-correlation between wavelet coefficients obtained from a $1/f$-type process generated using Keshner's synthesis. In this simulation, a 65,536-sample segment of a $1/f$ process was generated for $\gamma = 1$ and analyzed using Daubechies 5th-order wavelet basis. Here the sample-correlation function

of the coefficients at each scale was computed and averaged appropriately with the sample-correlation functions at the other scales. That the experimental result so closely matches the exact result for the bandlimited basis suggests that the analysis result for the bandlimited basis may, in fact, be more broadly applicable.

Before concluding this analysis section, it is appropriate to point out that several of the results we have described herein have been derived independently for the particular case of fractional Brownian motion using a time-domain approach. For instance, the stationarity of the wavelet coefficients at a fixed scale was first established by Flandrin [44]; the interscale stationarity property was described by Flandrin [71] (after Vergassola and Frisch [72]). Likewise, the expression for the asymptotic rate-of-decay of correlation among wavelet coefficients is essentially the same as that first derived by Tewfik and Kim [73]. We also mention that Flandrin [71] is able to provide stronger statements about the correlation among wavelet coefficients of fractional Brownian motion for the specific case of the Haar wavelet basis. Finally, we remark that it ought to be possible to interpret the decorrelation results presented both here and in the works of the above authors in the context of related results that have emerged concerning the effectiveness of wavelet decompositions in decorrelating a broad class of smooth covariance kernels [74].

Finally, it is useful to remark that through the octave-band filter bank interpretation of wavelet bases we may view wavelet-based analysis as spectral analysis on a logarithmic frequency scale. The results of this section, together with our observations of the spectral characteristics of $1/f$ processes earlier in the chapter, suggest that this kind of spectral analysis is, in some sense, ideally matched to $1/f$-type behavior. In the final section of this chapter, we undertake such a log-based spectral analysis of some real data sets using wavelets and show additional evidence that such analysis is potentially both useful and important in these cases.

Experiments

In this section, we undertake a very preliminary investigation of the properties of wavelet coefficients derived from some physical data sets. In the process, we identify two instances of time series that would appear to be well modeled as $1/f$ processes. The first example involves economic data, and is depicted in Fig. 3.5. The second example involves physiological data, and is depicted in Fig. 3.6.

Focusing first on the economic data, Fig. 3.5 shows the time series corresponding to raw weekly Dow Jones Industrial Average data accumulated over the past approximately 80 years. As shown in Fig. 3.7(a), the sample-variance of wavelet coefficients from scale to scale obeys a geometric

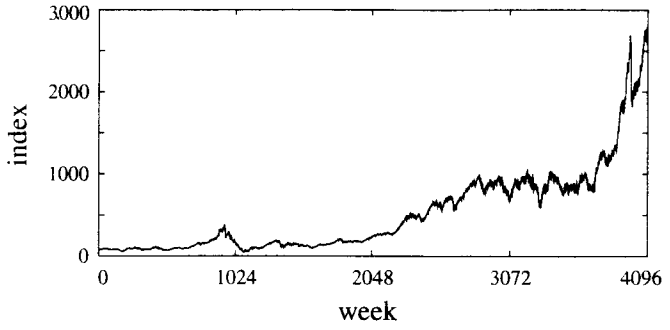

Figure 3.5. Weekly Dow Jones Industrial Average data, to present.

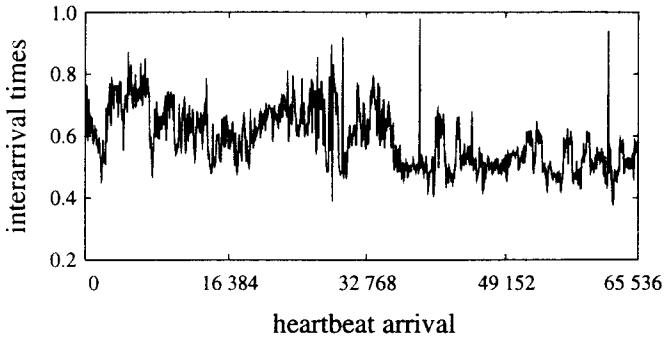

Figure 3.6. Heartbeat interarrival times for a healthy patient.

progression consistent with a $1/f$ process for which $\gamma \approx 2$. In Fig. 3.7(b), we see that the average along-scale sample-correlation among wavelet coefficients is rather weak. Since adjacent coefficients have a correlation of less than 8 percent, and more widely separated coefficients have a correlation of less than 3 percent, it would appear reasonable to neglect the intercoefficient correlation in the analysis of such data. While this behavior is also consistent with a $1/f$-type model for the data, we note that to justify such a model more fully, it would be necessary to study the correlation among coefficients between scales as well.

Turning our attention next to the physiological data, Fig. 3.6 shows a record of heart beat interarrival times for a healthy human patient corre-

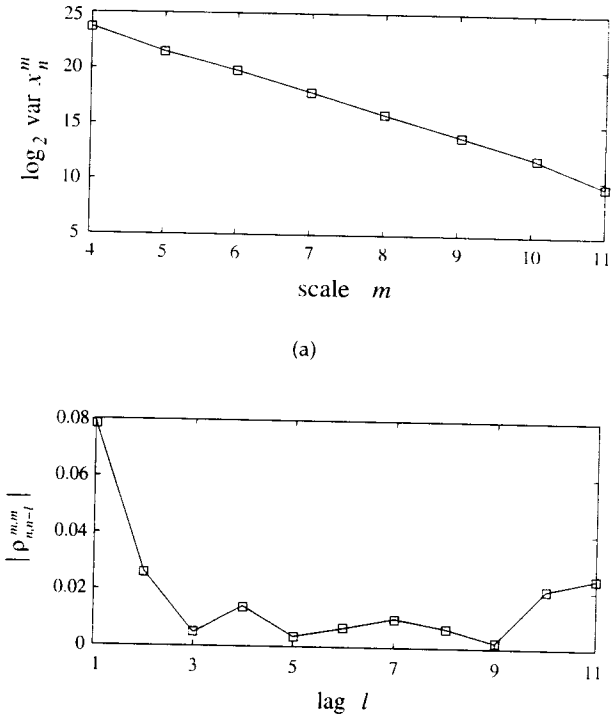

Figure 3.7. Wavelet-based analysis of weekly Dow Jones Industrial Average data. The time-series is analyzed using a 5th-order Daubechies wavelet basis. (a) Scale-to-scale wavelet coefficient sample-variance progression. (b) Average magnitude of the normalized along-scale sample-correlation between wavelet coefficients.

sponding to approximately 11 hours of continuously acquired data. The quantization levels of the interarrival times are spaced 4 milliseconds apart. In this example, as shown in Fig. 3.8(a), the sample-variances of wavelet coefficients from scale to scale obey a geometric progression consistent with a $1/f$ process of $\gamma \approx 1$. When viewing these progressions it is important to note that the number of samples available to make a variance estimate doubles at each successively finer scale. Hence, the standard deviation of the sample-variance measurement decreases by a factor of $\sqrt{2}$ for each successive increase in m. As a result, $1/f$ behavior manifests itself in the form

of log-variance characteristic that must be asymptotically linear in the limit of large m. In Fig. 3.8(b), we show the weak average along-scale sample-correlation between wavelet coefficients. In this case, coefficients separated by lags of two or more are correlated less than 2 percent, again suggesting that it is reasonable to neglect such intercoefficient correlation in any wavelet-based analysis. Again, we caution that no attempt was made to study the correlation structure among coefficients between scales.

3.4 SUMMARY

In this chapter, we focused our attention on fractal random processes having the key property that their statistics are invariant to temporal dilations and contractions of the process, to within an amplitude factor. Of particular interest were the $1/f$ family of such statistically self-similar random processes, and we developed some important new models for $1/f$-type behavior in signals. After reviewing the traditional fractional Brownian motion model for $1/f$ behavior, we developed a powerful alternative frequency-based characterization for $1/f$ processes. Here we showed that, although they are generally nonstationary, $1/f$ processes have the special property that when bandpass filtered they always produce stationary outputs.

In the second half of the chapter we relaxed our model constraints, and considered nearly-$1/f$ processes. We began by reviewing traditional ARMA models for nearly-$1/f$ behavior, then turned our attention to developing wavelet-based representations for $1/f$-type processes. As our main result we demonstrated that orthonormal wavelet basis expansions are Karhunen-Loève-like expansions for $1/f$-type processes, i.e., when $1/f$ processes are expanded in terms of orthonormal wavelet bases, the coefficients of the expansion are effectively uncorrelated. This result, which has powerful implications, was supported both theoretically and empirically, and we presented examples involving both simulated and real data.

Collectively, our theoretical and empirical results suggest that the orthonormal wavelet transform is an extremely useful and convenient tool in the synthesis and analysis of $1/f$-type processes. In the next chapter we explore how the wavelet transform plays an equally valuable role in the *processing* of such signals.